AIAA 99-0320

Regimes of Interaction Between a Nonpremixed Hydrogen-Air Flame and an Isolated Vortex

G. J. Fiechtner,[1,2] C. D. Carter,[1,2] V. R. Katta,[1,2]
J. R. Gord,[1] J. M. Donbar,[1] and J. C. Rolon[3]

[1]Air Force Research Laboratory
Wright-Patterson AFB, OH 45433-7103
[2]Innovative Scientific Solutions, Inc.
2766 Indian Ripple Road, Dayton, OH 45440-3638
[3]Laboratoire d'Énergétique Moléculaire et Macroscopique, Combustion, École Centrale Paris and CNRS, Grande Voie des Vignes 92295, Châtenay-Malabry Cedex, France

37th AIAA Aerospace Sciences Meeting and Exhibit
January 11-14, 1999 / Reno, NV

REGIMES OF INTERACTION BETWEEN A NONPREMIXED HYDROGEN-AIR FLAME AND AN ISOLATED VORTEX

G. J. Fiechtner,[1,4,5] C. D. Carter,[1,4] V.R. Katta,[1,4] James R. Gord,[2,4]
J. M. Donbar,[2,4] and J. C. Rolon[3]

Abstract

The dynamic interaction of a laminar flame and a vortex is examined. The hydroxyl (OH) layer produced by the flame is imaged using planar laser-induced fluorescence (PLIF), and vortex-characterization data are acquired using digital, two-color particle-image velocimetry (PIV). The PIV and PLIF measurements of OH are performed simultaneously. The hydrogen-air flame is supported in a nonpremixed opposed-jet burner. The apparatus is found to produce highly repeatable events, making it ideal for studying the interaction of a flame and an isolated vortex. A distinct annular extinction of the OH layer is observed, in good agreement with previous computational modeling predictions for the apparatus.

Introduction

Recent results in numerical modeling combined with experimental measurements have led to important advances in the understanding of combustion. Numerous investigations have contributed to these advances, including a particular type of study in which the interaction of a laminar, nonpremixed flame and a vortex is examined. These efforts involve repeatable, carefully controlled conditions that are highly amenable to experimental study. The resulting data can be used for a variety of purposes, such as identifying fundamental regimes of vortex-flame interactions (Renard et al., 1998a). This paper contains experimental results that are used to validate numerical computations.

In recent computational calculations, Katta (Katta et al., 1998) predicted that during the interaction of a nonpremixed hydrogen-air flame and an isolated vortex, the extinction of the OH layer would occur in an annular pattern. The experiments detailed in the present paper are performed to examine, in part, the validity of this prediction. Experimental results obtained with planar laser-induced fluorescence (PLIF) of OH are used to determine regimes in which the annular extinction occurs. The nonpremixed flame is supported by air and fuel in an opposed-jet burner. The fuel consists of hydrogen diluted with nitrogen. The amount of hydrogen in nitrogen is varied, along with the strength of the vortex. The temporal evolution of the vortex-flame interactions is imaged with the PLIF system. Additional measurements are performed to characterize the vortices. Particles are seeded into the flowfield, and the scattering is used for digital, two-color particle-image velocimetry (PIV) measurements. Digital PIV measurements are made simultaneously with PLIF measurements of OH.

Background

Numerous experimental studies of the interaction dynamics of vortices and flames have been conducted, and many of these investigations employed two-dimensional imaging to study the interaction. For premixed flame fronts, most measurements have been made using two types of flames. Hertzberg et al. (1984) and Escudie (1988) conducted an experiment in which a Karman vortex street was produced using a cylindrical rod in a cross flow of premixed gases. A V-flame was supported behind a wire positioned downstream of the rod that produced the vortex street. Planar tomographic imaging was used to study the interaction of the vortex street and the flame. A similar

[1]Air Force Research Laboratory, Wright-Patterson Air Force Base, OH 45433-7103, USA.

[2]Innovative Scientific Solutions, Inc., 2766 Indian Ripple Road, Dayton, OH 45440-3638, USA.

[3]Laboratoire d'Énergétique Moléculaire et Macroscopique, Combustion, École Centrale Paris and CNRS, Grande Voie des Vignes, 92295 Châtenay-Malabry Cedex, France.

[4]Member, AIAA.

[5]Corresponding author and presenter.

interaction of a Karman vortex street and a flame was investigated by Lee et al. (1993) using PLIF imaging of OH and by Nye et al. (1996) using both OH PLIF and PIV. A disadvantage of using the vortex street is the difficulty in isolating a single vortex. Samaniego (1992a) developed a means of injecting an isolated line vortex through a horizontal slot in the wall of a vertical wind tunnel; this was pursued as a means of replacing the vortex street in experiments with V-flames. A year later, Samaniego (1992b) presented results on the interaction of a line vortex and a V-flame. Schleiren images of the time-dependent vortex-flame interaction along with CH emission data from the entire flame were presented. Nguyen and Paul (1996) also studied vortex-flame interactions using the Samaniego burner, reporting results of PLIF measurements of OH and CH radicals.

In a second type of study involving premixed combustion, Jarosinski et al. (1988) studied a flame that was ignited at one end of a tube of premixed gases. A vortex was injected at the other end of the tube. The interaction dynamics were then photographed using a mercury-xenon arc lamp and a rotating-drum streak camera with a rotating-disc shutter. Recently, Driscoll and co-workers produced an impressive series of papers concerning a similar vortex-flame facility in which PIV, OH PLIF, or a combination of these imaging techniques was applied (Driscoll et al., 1994, Mueller et al., 1995; Mueller et al., 1996; Mueller et al., 1998; Roberts and Driscoll, 1991; Roberts et al., 1992; Roberts et al., 1993; Sinibaldi et al., 1998a; Sinibaldi et al., 1998b).

Nonpremixed flames have also been the subject of experimental study. Rolon and co-workers (Renard et al., 1998a; Renard et al., 1998b; Rolon et al., 1995; Thevenin et al., 1996; Thevenin et al., 1998) recently developed an apparatus in which a vortex is injected into a flame supported between the nozzles of an opposed-jet burner. This geometry has numerous advantages. First, unlike the above geometries, a stationary nonpremixed flame can be produced and isolated easily. Second, the flame thickness can be varied by changing either the nozzle velocities or the spacing between the upper and lower burner nozzles. The device has also been extended to the study of vortices that interact with premixed opposed-jet flames (Renard et al., 1998a). Takagi and coworkers (Takagi et al., 1996; Yoshida and Takagi, 1998) performed planar Rayleigh-scattering measurements of temperature in a similar type of opposed-jet burner in which a small jet of fuel or air was injected using a micro nozzle with an inner diameter of only 0.25 mm. Either a jet of air was injected from the air side of the diffusion flame or a jet of fuel was injected from the fuel side.

In a different class of measurements, Hsu et al. (1993) modulated the axial velocity of a laminar jet diffusion flame using a loud speaker to produce vortex-flame interactions. This apparatus was further studied by Hancock and coworkers (Hancock et al., 1996) using a number of techniques including reactive Mie scattering, PLIF, and digital PIV. These studies have provided large quantities of data for comparison with numerical-modeling predictions. A potential disadvantage of this burner is the complicated geometry (when compared to the above geometries, which involve completely isolated vortex injection) due to the convective velocity field associated with rotation of the vortex and translation of the flame zone. In a similar type of study, Mueller and Schefer (1998) recently performed OH PLIF measurements in a Wolfhard-Parker slot burner that was acoustically forced by loudspeakers on the side walls of the upstream fuel duct. PLIF imaging of acetone was used as a marker of the fuel.

More recently, Chen and Dahm (1998) developed a facility for generating a nonpremixed burning layer that wraps into a vortex ring. The facility permits experiments to be performed under conditions of both normal gravity and microgravity, allowing the study of the influence of buoyancy.

The experiments described in the present paper are based on the counterflow geometry of Rolon and co-workers (Renard et al., 1998a; Renard et al., 1998b; Rolon et al., 1995; Thevenin et al., 1996; Thevenin et al., 1998). A fuel mixture of hydrogen and nitrogen permits the use of laser diagnostics in the absence of hydrocarbon interferences, and the reaction zone of these nonpremixed flames is generally much thicker than that for premixed flames. Hydrogen chemistry simplifies the numerical calculations that are the subject of comparison with experimental results.

Apparatus and Procedure

Burner Facility

A picture (a) and diagram (b) of the Rolon burner are shown in Figure 1. The flame is supported between upper and lower nozzles separated by 40 mm, each with an exit diameter of 25 mm. The fuel consists of hydrogen diluted with nitrogen and flows from the upper nozzle. Air flows from the lower nozzle. Unique to this type of apparatus is a tube with 5-mm inner diameter that is installed concentrically within the lower nozzle. This tube is attached to a cylinder that contains a piston which, in turn, is attached to an actuator. Feeding an appropriate current to the actuator causes a solenoid to force the piston upward abruptly, resulting in the emergence of a vortex from the tube. For a cylindrical volume of fluid that emanates from a nozzle having length L and diameter D, Gharib et al. (1998) have shown that the maximum circulation which a vortex ring can attain is reached for L/D at ~4 and that

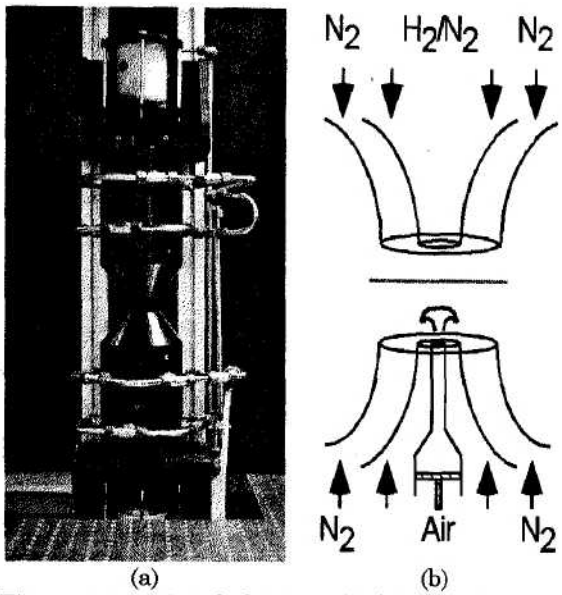

(a) (b)

Figure 1: (a) Digital photograph of opposed-jet burner. (b) Cross-sectional diagram of burner nozzles and piston.

for larger ratios additional trailing vortex rings form. For the present 0.5-cm nozzle, the volume that a vortex can contain as estimated from the results of Gharib et al. (1998) is ~0.4 cm^3. The present vortex generator can sweep a maximum volume of ~3 cm^3, for a maximum attainable *L/D* ratio of ~30. For the experiments described in this paper, comparatively strong vortices are generated using a 0.1-ms piston risetime. The piston is allowed to travel through its maximum range, but the tube is placed such that the diagnostics are triggered before a secondary or tertiary vortex exits the tube. The resulting leading vortex travels upward within the surrounding oxidizer flow. A flow of air is supplied to the vortex tube such that in the absence of a vortex, the exit velocity matches the velocity of the air from the surrounding nozzle. To minimize the impact of room-air disturbances, upper and lower guard flows of nitrogen are supported through outer nozzles, which are concentric with the respective upper and lower inner nozzles that support the flame.

The hydrogen, nitrogen-diluent, and oxidizer-air flows are furnished by mass-flow controllers with respective full-scale ranges of 20, 20, and 30 l/min. A continuous flow of air is provided to the vortex tube by a 5-l/min controller, while the guard flows for the upper and lower guard (outer) nozzles are furnished by two 50-l/min mass-flow controllers. The flow rates of the controllers are accurate to ±1% of the full-scale range. The experiments have been repeated for six flame conditions, as summarized in Table I.

Seed particles are introduced into the burner flows when digital PIV measurements of the vortex velocity are performed. Three particle seeders are

Table I: Flow rates (l/min) at 21.5°C and 724 mm Hg for six flame conditions. X_{H2} is the volume fraction of hydrogen in nitrogen diluent.

	Flame					
Gas	A	B	C	D	E	F
H_2	2.76	3.40	4.04	4.67	5.31	5.94
N_2	17.1	17.1	17.1	17.0	17.0	16.9
X_{H2}	0.14	0.17	0.19	0.22	0.24	0.26
Air	11.2	11.2	11.2	11.2	11.2	11.2

installed; one is placed after the air mass-flow controller, another after the vortex-air mass flow controller, and a third after the junction where the hydrogen and nitrogen gases are mixed. With the use of three seeders, each flow can be seeded with particles individually, or combinations of the different flowfields can be seeded. Each seeder contains hollow spherical ceramic particles with an approximate mean diameter of 2.4 μm. When PIV studies are not required, the seeders are removed from the apparatus.

Laser Diagnostics: OH PLIF Imaging

The PLIF system contains a frequency-doubled, Q-switched Nd:YAG laser that is used to pump a dye laser which, in turn, is frequency doubled. The UV radiation is directed through a telescope that is adjusted to produce a light sheet with a height that matches as nearly as possible the 40-mm burner separation. The resulting beam thickness is ~300 μm, which corresponds to the full width (defined as the distance between the locations of the 25% peak intensity points).

Hydroxyl radicals absorb the laser radiation at 281.3414 nm via the $R_1(8)$ transition of the (1,0) band in the A-X system. Fluorescence from the A-X (1,1) and (0,0) bands is detected at right angles through WG-295 and UG-11 colored-glass filters, using a 105-mm-focal-length f/4.5 UV lens. The resulting light is recorded on an intensified CCD camera with an intensifier gate width of 100 ns. CCD pixels are binned in 2 x 2 groups, resulting in an effective array size of 288 x 192 pixels, with an imaged area of 25.6 x 38.4 mm^2. The bottom of the image is 0.25 mm above the surface of the lower nozzle. A color table is used with a maximum value set to 95% of the maximum signal for all images taken at a given flame condition. The low-signal color is assigned by calculating the background noise and selecting a minimum value that is two standard deviations above this level. Therefore, in cases where "extinction" of the OH layer is observed, "extinction" refers to signal levels that fall below this minimum value and are, therefore, assigned the last color in the table. All images represent the signal collected during a single laser shot, and no smoothing of the resulting images is attempted.

In studies of vortex-flame interactions conducted by other investigators [see, for example, Najm et al. (1998)], LIF was applied as a marker of some other quantity such as heat release or burning rate. In the present experiments, the OH image is obtained for direct comparison with numerical computations of the OH distribution (Katta et al., 1998); therefore, no attempt is made to correlate the images with any other quantities, although it has recently been shown that the OH concentration may be a good indicator of flame extinction in this configuration (Renard et al., 1998b).

Laser Diagnostics: Digital, Two-Color PIV

Measurements of the velocity field are carried out using digital, two-color PIV (Gogenini et al., 1998a; Gogenini et al., 1998b; Donbar, 1998). Here, a color digital CCD (Khosla, 1992) with an array of 3060 x 2036 pixels is used. A magnification of 78,368 pixels/m is employed, resulting in an imaged area of 26.0 x 39.0 mm^2. The color CCD camera and the intensified CCD array are aligned using a transparent mask printed with a graduated scale. Further alignment between images is performed after each experiment employing software; a transformation in two-dimensional space is applied to the PIV images relative to the PLIF images. Two lasers are used, with one PIV light sheet produced by directly doubling the output of a Q-switched Nd:YAG laser (30 mJ/pulse at the test section). The remainder of this beam is used to pump the dye laser that is frequency doubled to excite OH fluorescence. The second PIV light sheet is produced by pumping a dye laser (employing DCM laser dye) with a second frequency-doubled, Q-switched Nd:YAG laser, resulting in laser radiation at 640 nm (40 mJ/pulse at the test section). The thickness of both the red and green light sheets is set to ~700 μm at the probe region. A digital delay generator is used to drive the timing of the two lasers such that the red pulses are delayed precisely with respect to the green ones. In the absence of a vortex, the underlying counterflow velocity field is probed with red pulses that are delayed by up to 1 ms with respect to the corresponding green pulses. For the fastest vortices studied, the delay between red and green pulses is reduced to 10 μs. The camera shutter is set to open for 1/15 s to permit both laser pulses to be detected by the color CCD. Most of the flame emission and light from other devices in the laboratory (monitors, etc.) is greatly attenuated by the shutter.

Velocity vectors are calculated using the correlation software described by Gogenini et al., (1998a). A correlation area of 128 x 128 pixels is used in the calculation, corresponding to a correlation area of 0.269 cm^2 and a spatial resolution of 1.6 mm. In these preliminary studies, the main interest in digital PIV measurements is to obtain the propagation velocity of the vortex, and this correlation area is acceptable for such purposes. We have also obtained acceptable results using correlation areas as small as 32 x 32 pixels, which will be utilized in future studies in which quantities such as strain will be calculated. Neighboring correlation boxes are overlapped by 75%, resulting in a velocity field with an area containing 95 x 60 vectors, or 5700 total vectors over the area of the color CCD. In some portions of each image, a small percentage of errant vectors results from low seed levels, scattering of light into the camera, flame emission, and other effects. Because the vortex-flame interactions are repeatable, digital PIV images can be recorded until an image with an extremely small percentage of incorrect vectors is obtained. For this reason, nearly 15 gigabytes of digital color image data were acquired.

Characterization of vortices is illustrated in Figure 2; a single, idealized vortex ring is superimposed over an axisymmetric cylindrical coordinate system using the coordinates z and u to illustrate the forward position and velocity, respectively. The coordinates r and v represent the radial position and velocity, respectively. In this coordinate representation. the vorticity simplifies to

$$\bar{\zeta} = \Delta \times \bar{V} = \frac{\partial v}{\partial z} - \frac{\partial u}{\partial r}. \qquad (1)$$

In these preliminary studies, evaluation of the derivatives in Eq. (1) is carried out without smoothing of the velocity field. Because this can cause amplification of noise, future calculations will be performed using an appropriate smoothing algorithm (Luff et al., 1996; Luff et al., 1998). When the velocity field represents the final desired result from reduction of digital PIV images, it is common to filter out incorrect vectors; this results in "holes" in the field that must be filled using a variety of techniques such as interpolation (Gogineni et al., 1998b). However, the resulting interpolated holes

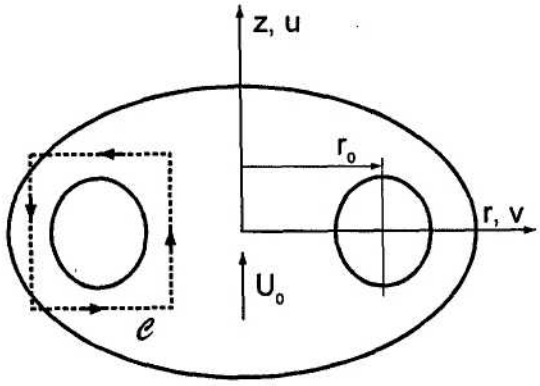

Figure 2. Coordinate system and integration contour used during computation of vortex properties (Daily and Harleman, 1966; Fox and MacDonald, 1985; Sullivan et al., 1973a; Sullivan et al., 1973b).

will represent a source of significant error in vorticity computations (Luff et al., 1996; Luff et al., 1998). Therefore, images with more than a few holes are discarded before attempts are made to compute the vorticity. In the future, an optimum method of computing the velocity field will be implemented to reduce the uncertainty in vorticity produced by the holes. Before images of vorticity are plotted, a 3 x 3 smoothing function, that is provided with the commercially available Transform® software, is applied four times. In these preliminary studies, the resulting images are used to examine the relative distribution of vorticity as a vortex propagates upward from the lower nozzle. In future studies in which the influence of the flame on the vorticity will be examined and quantitative vorticity information extracted, a more accurate method of computing and displaying the vorticity will be implemented (Luff et al., 1996; Luff et al., 1998).

The vortex circulation is computed using the integral over the contour shown in Figure 2 (Sullivan et al., 1973a; Sullivan et al., 1973b), yielding (Fox and MacDonald, 1985; Daily and Harleman, 1966; Luff et al., 1996; Luff et al., 1998)

$$\Gamma = \oint_e \vec{V} \bullet d\vec{s} = \sum_i \sum_j \vec{V}_{ij} \bullet \vec{s}_{ij} = \sum_i \sum_j \zeta_{ij} A_{\text{cell}} \qquad (2)$$

where C represents a contour box whose sides are drawn along lines where the vorticity remains below ~10% of its peak value (found at the core). The line-integral method (first double summation) and the vorticity-integral method (second double summation) are found to agree within 20%. To confirm the choice of contour and the integration process, the integration is performed over each side of the vortex depicted in Figure 2, and the resulting sum is determined to approach zero.

Planar Rayleigh Scattering

The above analysis of velocity fields has been used to estimate the forward propagation velocity of vortices or to compute vorticity in cold flows. Recent efforts have been made to examine digital, two-color errors in PIV results because of thermophoresis, which has the greatest influence for injection of comparatively slow vortices and for counterflow flames without vortex injection (Gomez and Rosner, 1993; Nichols, 1986; Pellet et al., 1995, Sung et al., 1994 and 1996; Talbot et al., 1980; Waldmann and Schmitt, 1980; and PIV data in greater detail, including calculations of vorticity, strain, etc., in the vicinity of the flame front. Unfortunately, sharp temperature gradients can cause Walsh, 1976). Knowledge of the temperature field would enable reduction of the velocity error introduced by thermophoresis. In addition, measurement of the temperature field would be advantageous for comparison with numerical computations. Because point temperature measurements would be extremely cumbersome in the present experiments, recent implementation of planar thermometry by Rayleigh scattering has been explored. Based on experimental observations of other researchers (Dibble and Hollenbach, 1980; Everest 1994; Everest et al, 1995; Komiyama et al., 1996, Takagi et al., 1996; and Yoshida and Takagi, 1998), Rayleigh scattering thermometry should be an excellent diagnostic for studies of vortex-flame interactions in the Rolon burner. In addition, the planar Rayleigh scattering signal can be collected using unintensified CCD cameras, allowing extended linear range and improved spatial resolution (Paul et al, 1990; Paul, 1991; and Williams et al, 1995).

Rayleigh scattering images are collected using a thinned, back-illuminated CCD with an image area of 550 x 550 pixels. The digital color camera is removed to make room for this CCD. Doubled Nd:YAG pulses of 400 mJ are scattered off the burner gases, and the scattering is directed through a four-cavity, 10-nm bandpass filter with a central wavelength of 532 nm. The bandpass filter is required to remove almost all background flame emission and synchronous fluorescence and scattering from simultaneous PLIF measurements of OH. The Rayleigh cross section is calibrated by passing Helium through the burner nozzles at room temperature and recording a scattering image. Next, room-temperature nitrogen is fed to the burner nozzles, and a scattering image is recorded. Because Rayleigh scattering data have only recently been collected, no images have been converted from pixel counts to temperature. Instead, each pixel is normalized to the scattering image of room-temperature nitrogen.

Synchronization and Timing

Precise synchronization of several experimental events is required, including vortex generation and propagation, production of laser pulses, and activation of the camera shutter and intensifier. Figure 3 contains a block diagram of the synchronization scheme.

Because the Nd:YAG lasers are designed to operate at a nominal repetition rate of 10 Hz, the experimental sequence must be synchronized to a 10-Hz master clock that drives the flash lamps and the Pockels cells of the lasers. To trigger the lasers, the clock sends two signals—one traveling to a 50-Ω power combiner and then to the laser digital delay generator (DDG). The 10-Hz clock also provides a TTL signal to one of two inputs of a coincidence unit. The second input of this unit is driven by a TTL pulse from the PLIF camera controller. The coincidence unit outputs a pulse only when pulses from both the 10-Hz clock and the PLIF camera controller are present. When a vortex-flame event is initiated using a personal computer, the PLIF

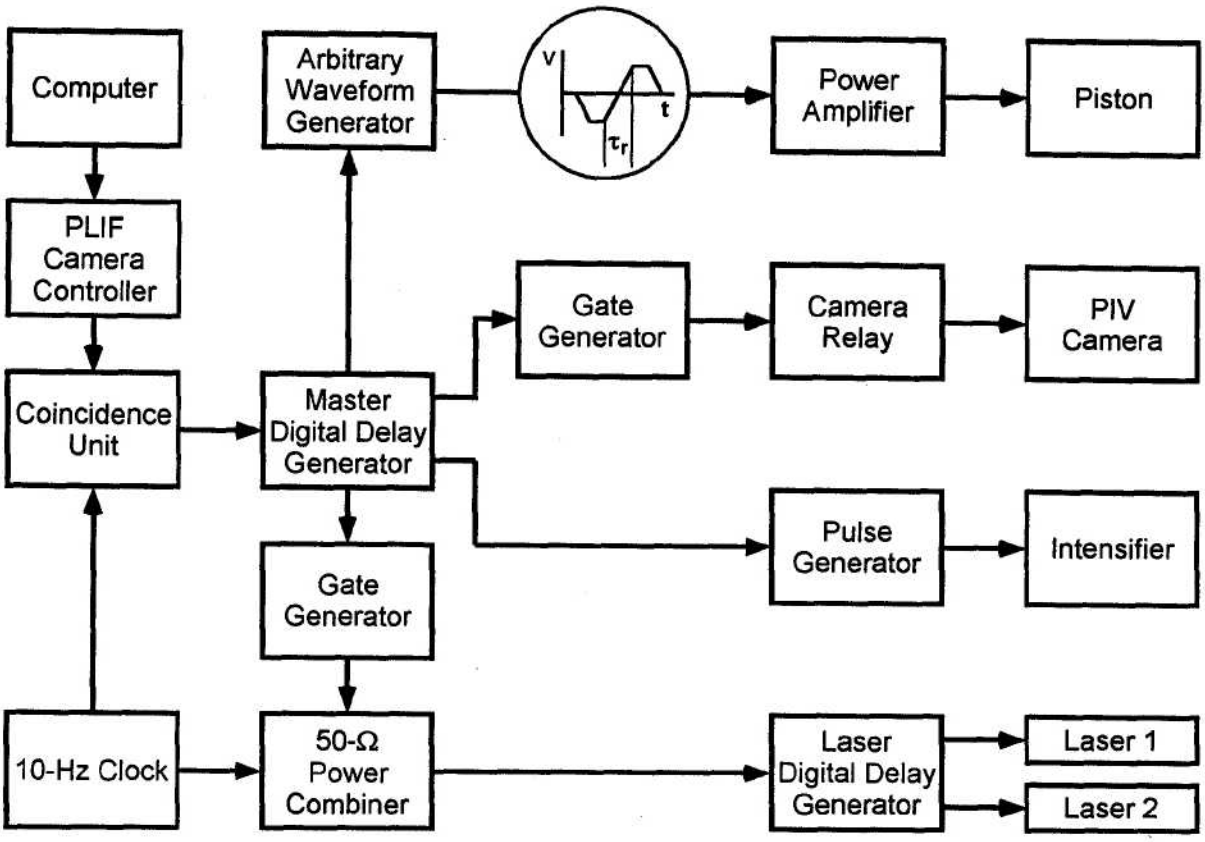

Figure 3: Diagram of electronic timing connections for simultaneous OH PLIF, digital PIV, and Rayleigh scattering measurements.

camera controller outputs a pulse ~1.3 s in duration. The corresponding output of the coincidence unit is a 1.3-s envelope of TTL pulses separated by 100 ms. The first pulse in this envelope triggers a master DDG, synchronizing it with the 10-Hz clock and the laser pulse train. This DDG triggers an arbitrary-waveform generator (AWG) that outputs a 1-s waveform; this waveform is amplified and fed to the piston actuator to generate a vortex. Approximately 0.5 s after the AWG waveform is initiated, the vortex is fired; therefore, five laser pulses are generated during the time between computer initiation and the vortex-flame interaction.

When the DDG is externally triggered, the jitter between the trigger and a DDG output pulse is 60 ps plus the output delay divided by 10^8. Over the 0.5-s period between the first and fifth laser pulses, this corresponds to a jitter of 5.06 ns. The 10-Hz-clock jitter specifications are not nearly so good. The jitter between clock outputs is one part in 10,000, corresponding to a jitter of 50 μs over the same 0.5-s period. Attempting to synchronize the piston with the clock severely limits the temporal resolution available to "freeze" vortex-flame events in time and requires an intensifier gate width significantly larger than 50 μs. The master DDG is, therefore, configured to trigger the fifth laser pulse preemptively. A delayed pulse from the master DDG arrives at the 50-Ω power combiner just before the fifth pulse in the clock pulse train, preemptively triggering the laser(s). If no initiation pulse is output from the computer, the laser(s) are triggered by the 10-Hz clock as usual. This approach reduces the jitter in the timing of the fifth laser pulse from 50 μs to ~5 ns while maintaining the nominal 10-Hz repetition rate required by the lasers.

Other outputs of the master DDG are suitably delayed and directed to the image detectors. For PIV experiments, the width of a TTL pulse is adjusted using a gate generator, which closes a relay to trigger the digital PIV camera system. For simultaneous PLIF experiments, another master-DDG output triggers a pulse generator which, in turn, activates the intensifier of an ICCD camera.

The scheme depicted in Figure 3 provides precise control of the relative timing between the laser diagnostics and the vortex-flame event. To explore the temporal evolution of the event, data are captured utilizing the following phase-locked timing sequence: 1) an image is recorded, 2) the delay between vortex

production and the laser/camera events is adjusted, and 3) another vortex is initiated and a second image recorded. This process is repeated to acquire numerous images, obtained at increasing delays; then an animation is created by assembling the individual images in temporal order. Effective temporal separation between images is selected between 10 and 200 μs, depending on the time scale of the event under study. The resulting animations are a testament to the high degree of repeatability achievable with this apparatus.

Results and Discussion

Vortex Characterization

Figure 4 shows the scattering signal obtained when the vortex-tube flow is seeded with a slightly higher particle density than that produced by the upper and lower burners. The corresponding set of vectors is shown at the right in Fig. 4. The vector field contains only six positions from a total of 5700 vectors where the software cannot be used to assign a velocity. The maximum vector length in the forward direction yields a propagation velocity of 0.77 m/s in this case.

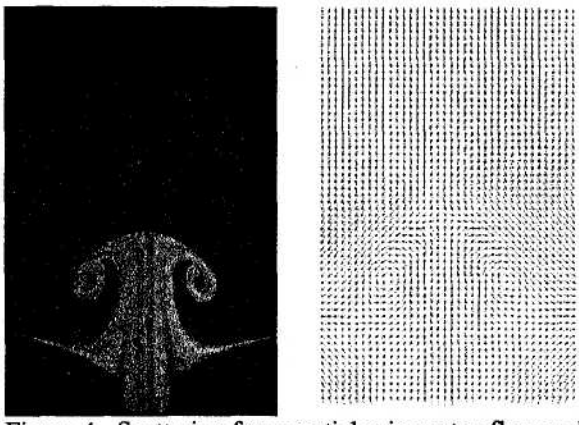

Figure 4. Scattering from particles in vortex flow and vectors calculated from scattering image.

The high quality of the velocity data enables the calculation of flowfield quantities such as vorticity. the temporal evolution of three different vortices is shown in Figure 5 using plots of vorticity fields. A "weak," an "intermediate," and a "strong" vortex are shown in rows (a), (b), and (c), respectively. The weak vortex has a circulation of ~76 cm^2/s and an initial propagation velocity of 1 m/s. However, the propagation velocity of this vortex slows to only 0.6 m/s by the fifth frame (labeled "50 ms"). Meanwhile, the separation between cores is 7 mm in the first frame (labeled "0 ms") and increases to nearly 15 mm in the fifth frame.

In contrast, the intermediate vortex shown in row (b) of Figure 5 has a circulation of 170 cm^2/s and an initial propagation velocity of 2.2 m/s. By the time the vortex reaches the position shown in the fifth frame of row (b), the propagation velocity has decreased to 1.8 m/s. The intermediate vortex shown in the first frame of row (b) has a core separation of 7.8 mm, which

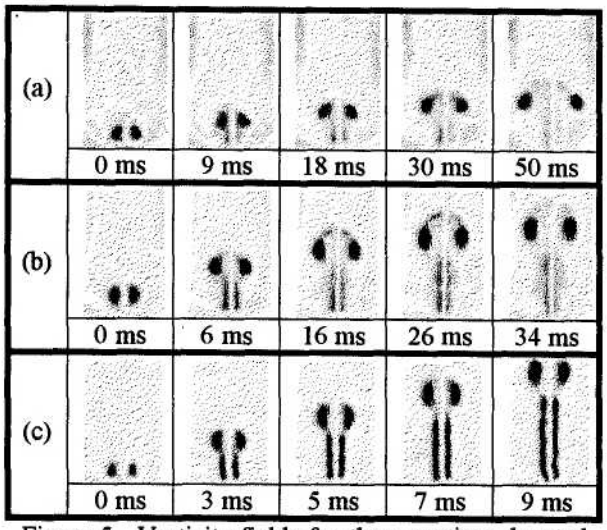

Figure 5. Vorticity fields for three vortices denoted by (a), (b), and (c). Times correspond to delays between the laser diagnostics trigger and the piston trigger.

increases to 12 mm by the fifth frame of row (b). Row (c) contains the time-resolved vorticity field for a "strong" vortex, which has a circulation of 1200 cm^2/s. This vortex has a propagation velocity of 8.4 m/s in the first frame. The velocity increases to a value of 10 m/s in the fourth frame and then decreases to 9.5 m/s in the fifth frame of row (c). The strong vortex has a core separation of 8 mm in the first frame, and the diameter grows to a value of 10.5 mm by the fifth frame of row (c). The strong vortex is observed to enter the upper-burner nozzle after the fifth frame. Care must be taken when attempting to generate a vortex that is stronger than case (c) since a three-dimensional lobe structure may result (Widnall, 1975).

Regimes of Flame-Vortex Interaction

The PLIF images of OH shown in Figure 6 correspond to a flame-vortex interaction in which extinction of the OH layer is absent. Initially, the vortex creates a small dent in the flame, and this dent then grows. Eventually the flame nearly surrounds the advancing vortex as it approaches the upper nozzle. In the later interaction stages, the OH PLIF signal level is observed to increase by greater than a factor of five over the levels observed without a vortex. The increased signal level is indicated by the light colors in the frames of Figure 6. This change in OH signal level is thought to indicate enhanced burning. For this particular example, the flow rates of Flame D in Table I are used.

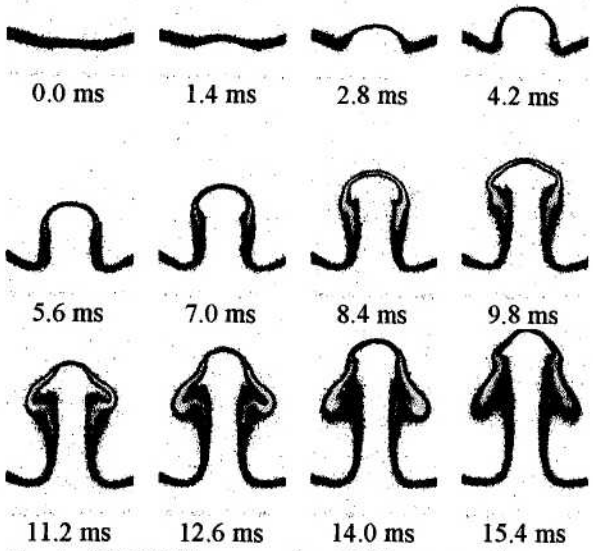

Fig. 6. OH PLIF images when OH layer remains intact.

The images of Figure 7 are obtained with flow conditions corresponding to Flame E in Table I and a vortex that is considered to be "strong". Extinction of the OH layer takes place in an annular pattern around the sides of the vortex, leaving a burning layer at its leading edge. This behavior was first predicted numerically by Katta,[1] well before these experiments were initiated, attesting to the utility of his code. After extinction, the isolated island of flame burns away, and the vortex travels upward toward the other nozzle. The flame follows the vortex, traveling up the stem. As the flame overtakes the vortex, it wraps up and turns in upon itself.

Typical planar Rayleigh-scattering images are shown in Figure 8. The flame conditions are similar to those for Figure 7; however, the vortex strength has been decreased slightly. As shown, Rayleigh-scattering images indicate an isolated island of high-temperature gas in front of the advancing vortex. Eventually this island burns around the vortex, and the island flame again contacts the outer flame at the vortex stem.

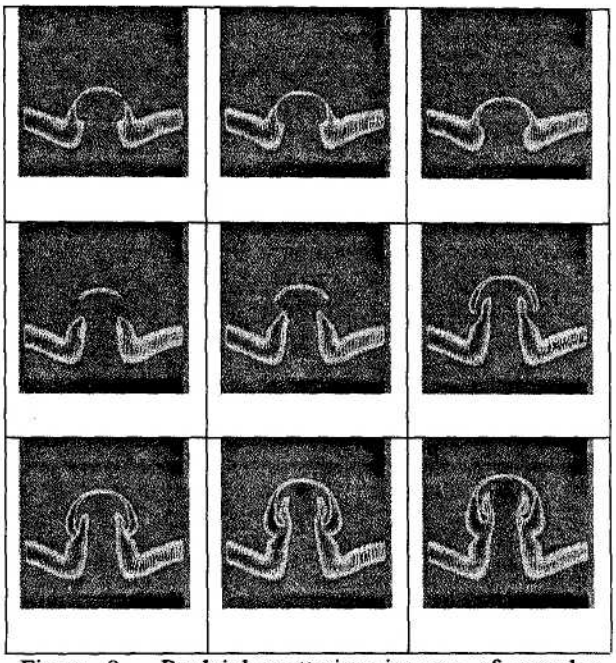
Figure 8. Rayleigh-scattering images of annular

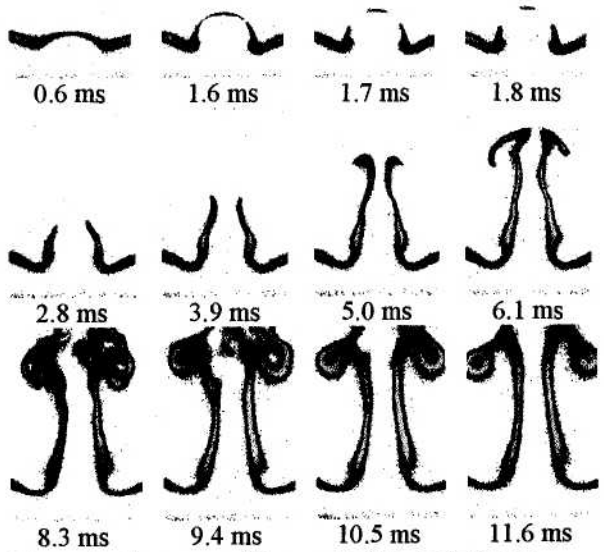

Figure 7: Sequence of images before and after extinction of the OH layer.

Future Investigations

Based on the success of the studies described in this paper, we plan to extend experiments in several ways. First, although the agreement between the computations and the experiments regarding the annular extinction is good, more extensive measurements will be taken to identify a cause for this phenomenon. For instance, the extinction pattern may result from a flowfield boundary condition that is peculiar to this particular apparatus. Indeed, an advantage of the model of Katta is that the vortex-injection boundary conditions can be included in the numerical-solution process. In addition, a more fundamental interaction, such as preferential diffusion (Yoshida and Takagi, 1998) may cause this phenomenon.

Second, the Rolon burner configuration may prove to be ideal for studying other interactions of importance to combustion. One example that we have

recently begun to study is the behavior of fire suppressants injected into a laminar hydrocarbon flame. Here, the vortex-injection tube is fitted with a three-way solenoid valve having two inlets. The first inlet provides the air flow described in this paper. The second inlet provides some other gas mixture or a droplet-containing flow. The current to the solenoid valve is timed such that it switches to the second inlet only for a period of time sufficient to fill the vortex tube. The piston is then triggered to produce a carefully-controlled vortex or jet. The interaction with the flame is monitored using the diagnostics described in this paper.

Finally, the measurement techniques are being improved to aid in interpretation of the data. For example, simultaneous acquisition of PLIF and PIV data enables careful examination of quantities such as flame stretch by overlapping images from two cameras. An image containing overlapped vectors and a PLIF image of OH is shown in Figure 9. These vectors were calculated using an effective spatial resolution of ~1.6 mm, which may be inadequate for spatial derivatives in the vicinity of the flamefront. We are presently working to improve the spatial resolution. More importantly, thermophoresis may introduce a bias into velocity vectors where temperature gradients are large (Gomez and Rosner, 1993; Sung et al, 1996). Using simultaneous PLIF and Rayleigh-scattering measurements, we hope to use overlapped flame fronts to overlap corresponding velocity and temperature fields. The resulting images should permit an examination of thermophoretic bias on the velocity field.

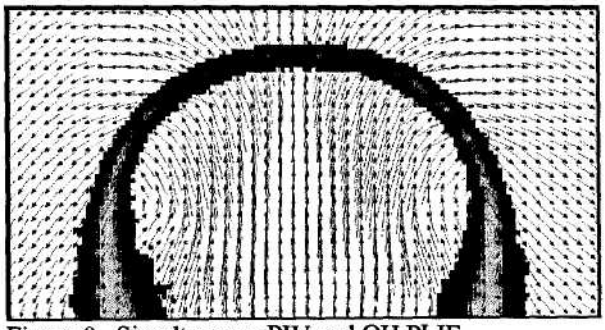

Figure 9. Simultaneous PIV and OH PLIF.

Conclusions

The apparatus of Rolon and co-workers (Renard et al., 1998a; Renard et al., 1998b; Rolon et al., 1995; Thevenin et al., 1996; Thevenin et al., 1998) has been implemented to study the interaction of a vortex and a flame. Digital two-color PIV has been applied to characterize the vortices injected into the opposed-jet flow. PLIF images of OH have been used to observe the dynamics of the interaction of the vortex and the flame. An annular break in the OH layer has been observed, in excellent agreement with the numerical computations of Katta (Katta et al., 1998).

Acknowledgements

The authors thank Mr. K. D. Grinstead, Jr., for technical assistance in setting up the experiments. The authors also acknowledge the advice of Drs. L. P. Goss, S. P. Gogineni, J. Estevadeordal, M. A. Linne, and Mr. T. Drouillard concerning the reduction of two-color PIV data. The authors thank Dr. R. D. Hancock and Lt. I. Vihinen for assistance in assembly and construction of the burner. The authors also acknowledge Mr. P.-H. Renard, Drs. R. D. Hancock, W. M. Roquemore, and K.-Y. Hsu for the stimulating discussions of vortex-flame dynamics. Finally, the authors wish to thank Ms. M. M. Whitaker for editorial assistance. This work is supported by U. S. Air Force Contracts F33615-95-C-2507 and F33615-97-C-2702.

References

Brickman, D., and Ruddick, B., 1990, "The Behavior and Stability of a Lens in a Strain Field," *Journal of Geophysical Research*, Vol. 95, No. C6, pp. 9657-9670.

Chen, S.-J., and Dahm, W. J. A., 1997, "Vortex Ring/Diffusion Flame Interactions in Microgravity Conditions," Proceedings of the *Fourth International Microgravity Combustion Workshop*, Cleveland, OH, pp. 191-196. NASA Conference Publication No. 10191.

Chen, S.-J., and Dahm, W. J. A, 1998, "Diffusion Flame Structure of a Laminar Vortex Ring Under Microgravity Conditions," accepted for publication in *Twenty-Seventh Symposium (International) on Combustion*, The Combustion Institute, Pittsburgh, PA.

Daily, J. W., and Harleman, D. R. F., 1966, "Fluid Dynamics," Addison-Wesley Publishing, Reading, MA.

Dibble, R. W., and Hollenback, R. E., 1981, "Laser Rayleigh Thermometry in Turbulent Flames," *Eighteenth Symposium (International) on Combustion*, The Combustion Institute, Pittsburgh, PA, pp. 1489-1499.

Donbar, J. M., 1998, "Reaction Zone Structure and Velocity Measurements in Permanently Blue Non-premixed Jet Flames," Ph.D. Dissertation, University of Michigan, Ann Arbor, MI.

Driscoll, J. F., Sutkus, D. J., Roberts, W. L., Post, M. E., and Goss, L. P., 1993, "The Strain Exerted by a Vortex on a Flame – Determined from Velocity Field Images," AIAA Paper No. 93-0362.

Driscoll, J. F., Sutkus, D. J., Roberts, W. L., Post, M. E., and Goss, L. P., 1994, "The Strain Exerted by a Vortex on a Flame – Determined from Velocity Field Images," *Combustion Science and Technology*, Vol. 4/6, pp. 213-229.

Dritschel, D. G., 1989, "Strain-Induced Vortex Stripping," in *Mathematical Aspects of Vortex Dynamics*, R. E. Caflisch, ed., SIAM, Philadelphia, PA, pp. 107-119.

Escudie, D., 1988, "Stability of a Premixed Laminar V-Shaped Flame," *Progress in Astronautics and Aeronautics*, Vol. 113, pp. 215-239.

Everest., D. A., 1994, "The Effect of Strain Rate on the Temperature Field Structure in a Turbulent Non-Premixed Flame Using Planar Rayleigh Scattering," Ph.D. Dissertation, University of Michigan, Ann Arbor, MI.

Everest, D. A., Driscoll, J. F., Dahm, W. J. A., and Feikema, D. A., 1995, "Images of the Temperature Field and Temperature Gradients to Quantify Mixing Rates within a Non-Premixed Turbulent Jet Flame," *Combustion and Flame*, Vol. 101, pp. 58-68.

Fox, R. W., and McDonald, A. T., 1985, "Introduction to Fluid Mechanics," John Wiley & Sons, New York.

Frenklach, M., Wang, H., Goldenberg, M., Smith, G. P., Golden, D. M., Bowman, C. T., Hanson, R. K., Gardiner, W. C., Lissianski, V., 1995, *Gas Research Institute Technical Report* No. GRI-95/0058.

Gharib, M., Rambod, E., and Shariff, K., 1988, "A Universal Time Scale for Vortex Ring Formation," *Journal of Fluid Mechanics*, Vol. 360, pp. 121-140.

Gogineni, S., Goss, L. P., and Roquemore, W. M., 1998a, "Manipulation of a Jet in a Cross Flow," *Experimental Thermal and Fluid Science*, Vol. 16, pp. 209-219.

Gogineni, S., Goss, L., Pestian, D., and Rivir, R., 1998b, "Two-Color Digital PIV Employing a Single CCD Camera," *Experiments in Fluids*, in press.

Gomez, A., and Rosner, D. E., 1993, "Thermophoretic Effects on Particles in Counterflow Laminar Diffusion Flames," *Combustion Science and Technology*, Vol. 89., Nos. 5-6, pp. 335-362.

Hancock, R. D., 1996, "Laser Diagnostic Investigation of the Structure of Steady and Driven Hydrogen Jet Diffusion Flames," Ph.D. Dissertation, University of Illinois, Urbana.

Hancock, R. D., Schauer, F. R., Lucht, R. P., Katta, V. R., and Hsu, K. Y., 1996, "Thermal Diffusion Effects and Vortex-Flame Interactions in Hydrogen Jet Diffusion Flames," *Twenty-Sixth Symposium (International) on Combustion*, The Combustion Institute, Pittsburgh, PA, pp. 1087-1093.

Hancock, R. D., Schauer, F. R., Lucht, R. P., and Farrow, R. L., 1997, "Dual-Pump Coherent Anti-Stokes Raman Scattering (CARS) Measurements of Nitrogen and Oxygen in a Laminar Jet Diffusion Flame," *Applied Optics*, Vol. 36, No. 15, pp. 3217-3226.

Hertzberg, J. R., Namazian, M., and Talbot, L., 1984, "A Laser Tomographic Study of a Laminar Flame in a Karman Vortex Street," *Combustion Science and Technology*, Vol. 38, No. 3/4, pp. 205-216.

Hsu, K. Y., Chen, L. D., Katta, V. R., Goss, L. P., and Roquemore, W. M., 1993, "Experimental and Numerical Investigations of the Vortex-Flame Interactions in a Driven Jet Diffusion Flame," AIAA Paper No. 93-0455.

Jarosinski, J., Lee, J. H. S., and Knystautas, R., 1988, "Interaction of a Vortex Ring and a Laminar Flame," *Twenty-Second Symposium (International) on Combustion*, Pittsburgh, PA, pp. 505-514.

Katta, V. R., Goss, L. P., and Roquemore, W. M., 1994, "Numerical Investigations of Transitional H_2/N_2 Jet Diffusion Flames," *AIAA Journal*, Vol. 32, No. 1, pp. 84-94.

Katta, V.R., Carter, C. D., Fiechtner, G. J., Roquemore, W. M., Gord, J. R. and Rolon, J. C., 1998, "Interaction of a Vortex With a Flat Flame Formed Between Opposing Jets of Hydrogen and Air," accepted for publication in *Twenty-Seventh Symposium (International) on Combustion*, The Combustion Institute, Pittsburgh, PA.

Khosla, R. P., 1992, "From Photons to Bits," *Physics Today*, Vol. 45, No. 12, pp. 42-49.

Komiyama, M., Miyafuji, A., and Takagi, T., 1996, "Flamelet Behavior in a Turbulent Diffusion Flame Measured by Rayleigh Scattering Image Velocimetry," *Twenty-Sixth Symposium (International) on Combustion, The Combustion Institute*, Pittsburgh, PA, pp. 339-346.

Lee, T.-W., Lee, J. G., Nye, D. A., and Santavicca, D. A., 1993, "Local Response and Surface Properties of Premixed Flames During Interactions with Karman Vortex Streets," *Combustion and Flame*, Vol. 94, No. 1/2, pp. 146-160.

Legras, B., and Dritschel, D. G., 1993, "Vortex Stripping and the Generation of High Vorticity Gradients in Two-Dimensional Flows," *Applied Scientific Research*, Vol. 51, pp. 445-455.

Leonard, B. P., 1979, "A Stable and Accurate Convective Modeling Procedure Based on Quadratic Upstream Interpolation," *Computer Methods in Applied Mechanics and Engineering*, Vol. 19, pp. 59-98.

Luff, J. D., Rompage, A. M., Linne, M. A., and Hertzberg, J. R., 1996, "Uncertainties Associated with the Post-Processing of 2-D Particle Image Velocimetry (PIV) Velocity Data of Unsteady Flow Fields," presented at the *Spring Technical Meeting of the Western States Section/ The Combustion In-*

stitute, Tempe, AZ, March, 1996. Paper No. WSS 96S-005.

Luff, J. D., Drouillard, T., Rompage, A. M., Linne, M. A., and Hertzberg, J. R., 1998, "Experimental Uncertainties Associated with Particle Image Velocimetry (PIV) Based Vorticity Algorithms," to appear in *Experiments in Fluids*, Vol. 25.

Mariotte, A., and Legras, B., 1994, "Vortex Stripping and the Erosion of Coherent Structures in Two-Dimensional Flows," *Physics of Fluids*, Vol. 6, No. 12, pp. 3954-3962.

Mueller, C. J., Driscoll, J. F., Sutkus, D. J., Roberts, W. L., Drake, M. C., and Smooke, M. D., 1995, "Effect of Unsteady Stretch Rate on OH Chemistry During a Vortex-Flame Interaction: To Assess Flamelet Models," *Combustion and Flame*, Vol. 100, No. 1/2, pp. 323-331.

Mueller, C. J., Driscoll, J. F., Ruess, D. L., and Drake, M. C., 1996, "Effects of Unsteady Stretch on the Strength of a Freely-Propagating Flame Wrinkled by a Vortex," *Twenty-Sixth Symposium (International) on Combustion*, The Combustion Institute, Pittsburgh, PA, pp. 347-355.

Mueller, C. J., 1996, "Measurements of Vortex-Flame Interaction Dynamics and Chemistry," Ph.D. Dissertation, University of Michigan, Ann Arbor.

Mueller, C. J., Driscoll, J. F., Reuss, D. L., Drake, M. C., and Rosalik, M. E., 1998, "Vorticity Generation and Attenuation as Vortices Convect Through a Premixed Flame," *Combustion and Flame*, Vol. 112, No. 3, pp. 342-358.

Mueller, C. J., and Schefer, R. W., 1998, "Coupling of a Diffusion Flame Structure to an Unsteady Vortical Flowfield," accepted for publication in *Twenty-Seventh Symposium (International) on Combustion*, The Combustion Institute, Pittsburgh, PA.

Najm, H. N., Paul, P. H., Mueller, C. J., and Wyckoff, P. S., 1998, "On the Adequacy of Certain Experimental Observables as Measurements of Flame Burning Rate," *Combustion and Flame*, Vol. 113, No. 3, pp. 312-332.

Nguyen, Q.-V., and Paul, P. H., 1996, "The Time Evolution of a Vortex-Flame Interaction Observed via Planar Imaging of CH and OH," *Twenty-Sixth Symposium (International) on Combustion*, The Combustion Institute, Pittsburgh, PA, pp. 357-364.

Nichols, R. H., 1986, "The Effects of Particle Dynamics on Turbulence Measurements with the Laser Doppler Velocimeter," Ph.D. Dissertation, University of Tennessee, Knoxville, TN.

Nye, D. A., Lee, J. G., Lee, T.-W., and Santavicca, D. A., 1996, "Flame Stretch Measurements During the Interaction of Premixed Flames and Karman Vortex Streets Using PIV," *Combustion and Flame*, Vol. 94, No. 1/2, pp. 167-176.

Paul, P. H., 1991, "The Application of Intensified Array Detectors to Quantitative Planar Laser-Induced Fluorescence Imaging," AIAA 91-2315.

Paul, P. H., van Cruyningen, I., Hanson, R. K., and Kychakoff, G., 1990, "High Resolution Digital Flowfield Imaging of Jets," *Experiments in Fluids*, Vol. 9, pp. 241-251.

Pellet, G. J., Wilson, L. G., Humphreys, W. J., Jr., Batram, S. M., Gatrell, L. R., and Issac, K. M., 1995, "Velocity Fields of Axisymmetric Hydrogen-Air Counterflow Diffusion Flames from LDV, PIV, and Numerical Computation," AIAA 95-3112.

Renard, P.-H., Rolon, J. C., Thevenin, D., and Candel, S., 1998a, "Wrinkling, Pocket Formation and Double Premixed .Flame Interaction Processes," accepted for publication in *Twenty-Seventh Symposium (International) on Combustion*, The Combustion Institute, Pittsburgh, PA.

Renard, P.-H., Rolon, J. C., Thevenin, D., and Candel, S., 1998b, "Investigations of Heat Release, Extinction, and Time Evolution of the Flame Surface for a Non-Premixed Flame Interacting with a Vortex," accepted for publication, *Combustion and Flame*.

Roberts, W. L., and Driscoll, J. F., 1991, "A Laminar Vortex Interacting with a Premixed Flame: Measured Formation of Pockets of Reactants," *Combustion and Flame*, Vol. 87, No. 3/4, pp. 245-256.

Roberts, W. L., 1992, "A Premixed Laminar Flame Interacting With a Vortex Resulting in Flame Stretch and Quenching," Ph.D. Dissertation, University of Michigan, Ann Arbor, MI.

Roberts, W. L., Driscoll, J. F., Drake, M. C., and Ratcliffe, J. W., 1992, "OH Fluorescence Images of the Quenching of a Premixed Flame During an Interaction with a Vortex," *Twenty-Fourth Symposium (International) on Combustion*, The Combustion Institute, Pittsburgh, pp. 169-176.

Roberts, W. L., Driscoll, J. F., Drake, M. C., and Goss, L. P., 1993, "Images of the Quenching of a Flame by a Vortex – To Quantify Regimes of Turbulent Combustion," *Combustion and Flame*, Vol. 94, No. 1/2, pp. 58-69.

Rolon, J. C., Aguerre, F., and Candel, S., 1995, "Experiments on the Interaction Between a Vortex and a Strained Diffusion Flame," *Combustion and Flame*, Vol. 100, No. 3, pp. 422-429.

Samaniego, J.-M., 1992a, "Generation of Two-Dimensional Vortices in a Cross Flow," *Annual Research Briefs – 1992*, Center for Turbulence Research, NASA Ames Research Center/Stanford University, pp. 431-441.

Samaniego, J.-M., 1992b, "Stretch-Induced Quenching in Vortex-Flame Interactions," *Annual Research Briefs – 1993*, Center For Turbulence Research, NASA Ames Research Center/Stanford University, pp. 205-218.

Schauer, F. R., 1998, "Thermal Diffusion and Flame Structure in a Laminar Hydrogen Jet Diffusion Flame," Ph.D. Thesis, University of Illinois, Urbana.

Schauer, F. R., Hancock, R. D., Gogineni, S., and Lucht, R. P., 1998, "Vortex-Flame Interactions in Hydrogen Jet Diffusion Flames: A DPIV and DNS Investigation," submitted to *Experiments in Fluids*.

Sinibaldi, J. O., Mueller, C. J., and Driscoll, J. F., 1997, "Measured Local Propagation Velocities of Wrinkled Premixed Flames," Proceedings of the *Fall Technical Meeting*, The Eastern States Section of the Combustion Institute, Hartford, CT, pp. 179-182.

Sinibaldi, J. O., Driscoll, J. F., Mueller, C. J., and Tulkki, A. E., 1997 "Flame-Vortex Interactions: Effects of Buoyancy from Microgravity Imaging Studies," AIAA 97-0669.

Sinibaldi, J. O., Mueller, C. J., Tulkki, A. E., and Driscoll, J. F., 1998, "Suppression of Flame Wrinkling by Buoyancy: The Baroclinic Stabilization Mechanism," AIAA Journal, Vol. 36, No. 8, pp. 1432-1438.

Sinibaldi, J. O., Mueller, C. J., and Driscoll, J. F., 1998, "Local Flame Propagation Speeds Along Wrinkled, Unsteady, Stretched Premixed Flames," accepted for publication in *Twenty-Seventh Symposium (International) on Combustion*, The Combustion Institute, Pittsburgh, PA.

Sullivan, J. P., Widnall, S. E., and Ezekiel, S., 1973a, "Study of Vortex Rings Using a Laser Doppler Velocimeter," AIAA Paper No. 73-105.

Sullivan, J. P., Widnall, S. E., and Ezekiel, S., 1973b, "Study of Vortex Rings Using a Laser Doppler Velocimeter," *AIAA Journal*, Vol. 11, No. 10, pp. 1384-1389.

Sung, C. J., Law, C. K., and Axelbaum, R. L., 1994, "Thermophoretic Effects on Seeding Particles in LDV Measurements of Flames," *Combustion Science and Technology*, Vol. 99, pp. 119-132.

Sung, C. J., Kistler, J. S., Nishioka, M., and Law, C. K., 1996, "Further Studies on Effects of Thermophoresis on Seeding Particles in LDV Measurements of Strained Flames," *Combustion and Flame*, Vol. 105, pp. 189-201.

Takagi, T., Yoshikawa, Y., Yoshida, K., Komiyama, M., and Kinoshita, S., 1996, "Studies on Strained Non-Premixed Flames Affected by Flame Curvature and Preferential Diffusion," Twenty-Sixth Symposium (International) on Combustion, The Combustion Institute, Pittsburgh, PA, pp. 1103-1110.

Talbot, L., Cheng, R. K., Schefer, R. W., and Willis, D. R., 1980, "Thermophoresis of Particles in a Heated Boundary Layer," *Journal of Fluid Mechanics*, Vol. 101, No. 4, pp. 737-758.

Thevenin, D., Rolon, J. C., Renard, P.-H., Kendrick, D. W., Veynante, D., and Candel, S., 1996, "Structure of a Nonpremixed Flame Interacting with Counter-rotating Vortices," *Twenth-Sixth Symposium (International) on Combustion*, The Combustion Institute, Pittsburgh, PA, pp. 1079-1086.

Thevenin, D., Renard, P.-H., Rolon, J. C., and Candel, S., 1998, "Extinction Processes During a Non-Premixed Flame/Vortex Interaction," accepted for publication in *Twenty-Seventh Symposium (International) on Combustion*, The Combustion Institute, Pittsburgh, PA.

Trieling, R. R., Beckers, M., and van Heijst, G. J. F., 1997, "Dynamics of Monopolar Vortices in a Strain Flow," *Journal of Fluid Mechanics*, Vol. 345, pp. 165-201.

Trieling, R. R., van Wesenbeeck, J. M. A., and van Heijst, G. J. F., 1998, "Dipolar Vortices in a Strain Flow," *Physics of Fluids*, Vol. 10, No. 1, pp. 144-159.

Yoshida, K., and Takagi, T., 1998, "Transient Local Extinction and Reignition Behavior of Diffusion Flames Affected by Flame Curvature and Preferential Diffusion," accepted for publication in *Twenty-Seventh Symposium (International) on Combustion*, The Combustion Institute, Pittsburgh, PA.

Waldmann, L., and Schmitt, K. H., 1966, "Thermophoresis and Diffusiophoresis of Aerosols," in *Aerosol Science*, C. N. Davies, ed., Academic Press, New York, pp. 137-162.

Walsh, M. J., 1976, "Influence of Particle Drag Coefficient on Particle Motion in High Speed Flow with Typical Laser Velocimetry Applications," NASA TN D-8120.

Widnall, S. E., 1975, "The Structure and Dynamics of Vortex Filaments," *Annu. Rev. Fluid. Mech.*, Vol. 7, pp. 141-165.

Williams, G. A., Jr., Reihheimer, A. L., Johnson, C. B., Wheeler, K. D., Wodecki, N. D., Aebi, V. W., and Costello, K. A., 1995, "Back-Illuminated and Electron-Bombarded CCD's Low Light Level Imaging System Performance," SPIE Volume 2551, pp. 208-223.